Plastic bubbles and tamper $\langle \rho R \rangle$ measurements for laser-driven fusion experiments

Cite as: Journal of Applied Physics **47**, 1491 (1976); https://doi.org/10.1063/1.322814
Published Online: 28 August 2008

F. J. Mayer, and W. B. Rensel

Plastic bubbles and tamper $\langle \rho R \rangle$ measurements for laser-driven fusion experiments*

F. J. Mayer and W. B. Rensel

KMS Fusion, Incorporated, P. O. Box 1567, Ann Arbor, Michigan 48106
(Received 7 November 1975)

A new diagnostic technique is described which makes use of large-diameter (~ 5 cm) thin-walled (~ 10 μm) plastic bubbles to collect neutron-activated tamper material in a laser-driven fusion experiment. The plastic bubble and radioactive material are dissolved in a solvent and counted in a Čerenkov scheme to determine the average tamper $\langle \rho R \rangle$ at peak compression conditions. The bubble energy flow and other plasma diagnostic characteristics are also briefly discussed.

PACS numbers: 28.50.Re, 52.50.Jm, 52.70.—m

I. INTRODUCTION

The laser-driven implosion of DT gas-filled spherical glass-shell targets is now being actively pursued at KMS Fusion,[1] Lawrence Livermore Laboratory,[2] Los Alamos Scientific Laboratory,[3] and the University of Rochester.[4] These implosion experiments are testing the theoretical concepts behind the high-density laser-fusion inertial confinement scheme,[5,6] in which it is crucial to drive the imploded DT fuel to very high $\langle \rho R \rangle$ (mass density times fuel radius) values ($\rho R \approx 1$ g/cm^2) to obtain efficient thermonuclear burn.

This report describes one $\langle \rho R \rangle$ measurement technique which makes use of the neutron activation of target material (either an additive to the DT fuel[7] core or the pusher-tamper glass shell used in the present experiments). The concept of the technique is to simply collect the neutron-activated target material for radioactive analysis, after the laser-driven implosion experiment. This is accomplished by placing a thin (~ 1—20 μm) polyvinyl-acetate bubble of about 5 cm diameter around the glass-shell targets (typically ~ 50—100 μm in diameter). The laser radiation is transmitted through the bubble and focused onto the target, but the exploding target material is imbedded in the bubble which is then removed from the experimental chamber.

The plastic bubble (with imbedded target material) is then subjected to radioactive analysis to determine the amount of target activation produced.

In this paper, we describe the bubble technique, the activation analysis, and data reduction for the presently used glass-shell fusion targets. Some implications for target plasma diagnostics are also presented.

II. BUBBLE TECHNIQUE

The clear plastic bubbles for these experiments were fabricated from polyvinyl acetate using the techniques originally developed by Grosse.[8] Although much larger bubbles are possible, we were constrained to a diameter of about 4 cm by the width of the annular gap separating the two ellipsoidal mirrors used in the KMS Fusion illumination scheme.[9] Some relevant bubble characteristics are as follows: diameters from 300 μm to ~ 20 cm; wall thicknesses from 1 to 200 μm; specific gravity, 1.18; refractive index, 1.47; transmission at 1.06 μm ≥ 95%.

The bubbles were formed by blowing a viscous solution of polyvinyl-acetate plastic into a nearly spherical bubble of the desired diameter. Solid pellets of plastic were thoroughly dissolved in acetone to form a fairly dilute solution with low viscosity. The initial low viscosity permits the air bubbles entrapped during mixing to escape before the viscosity is reduced. Although a plasticizer could be used,[8] our relatively small bubbles, proved to be relatively rigid without it and not subject to distortion during target mounting and target chamber evacuation.

A blow pipe was fashioned from a short section of glass tubing by forming an open conical flange at one end and a small-diameter tip-off in the center [Fig. 1(a)]. The bubbles are formed by bringing the conical flange of the blow pipe barely in contact with the surface of the solution and drawing a quantity of the viscous solution into the cone. The blow pipe is withdrawn from

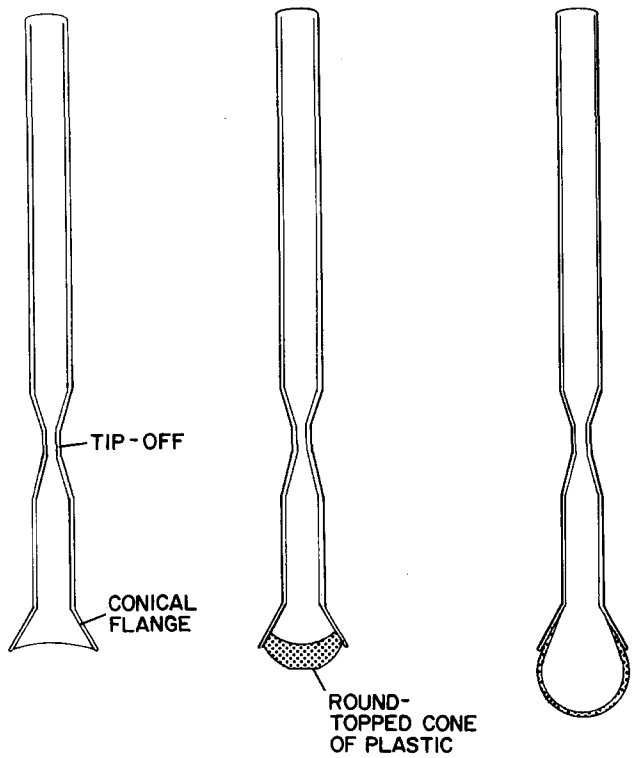

FIG. 1. Sketch of bubble blowing sequence.

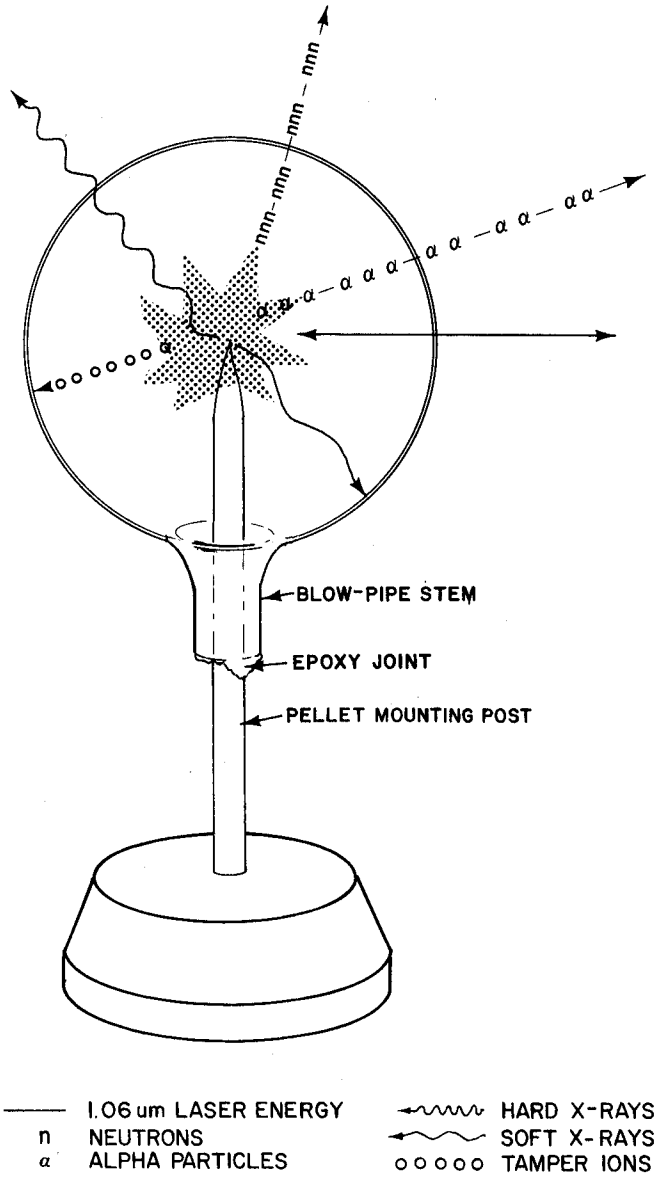

FIG. 2. Schematic of energy flow through bubble wall and target mounting.

the solution and the plastic filament that forms between the pipe and the viscous solution is cut near the pipe with a pair of scissors. The remove all traces of the scissor cut, the end of the pipe is lowered into a beaker of pure acetone and rotated at an angle against the side of the beaker to form a round-topped cone [Fig. 1(b)]. Air pressure very gently applied to the pipe will form a small thick-walled minishell [Fig. 1(c)]. This is the most difficult part of the process and requires care and some practice. Further expansion of the minishell can be accomplished in a number of partial expansions over a period of a few minutes.

The blow pipe is then sealed by heating with a small torch at the previously prepared tip-off section. The bubble should be allowed to dry in the bubble-down position until the plastic shell becomes fairly rigid. Most of the blow pipe may then be removed by scribing and breaking the pipe leaving a short open stem for handling and target mounting. The plastic sphere is next placed in a vacuum desiccator, still in the bubble-down position, to remove the remaining acetone solvent from the thin wall, causing it to become quite rigid.

A laser target[10] that has been previously characterized and mounted on a standard target post is inserted through the bubble stem and the target is positioned in the geometric center of the bubble. The target mounting post and the stem are secured together with a small quantity of epoxy glue (Fig. 2). If the inside diameter of the stem is slightly larger than the outside diameter of the target mounting post, the space between the two will allow removal of the gas from inside the bubble without shattering it when the target chamber is evacuated. Figure 3 is a photograph of the final bubble-target assembly mounted on a temporary base.

III. ENERGY TRANSMISSION CONSIDERATIONS

The energy flow into and out of the plastic bubbles is of importance when analyzing the laser fusion implosion experiment. Figure 2 shows schematically the transmission of the various energy components in the experiment.

The plastic bubbles, being of the order of the laser wavelength in thickness, do not introduce extreme optical defocusing effects. Furthermore, the polyvinyl acetate has good transmission (~95%) at 1.06 μm. Therefore, the bubble does not substantially change the 1.06-μm laser energy measurements (i.e., incident, reflected, and target-scattered energy[11]). The bubble is chosen large enough that the power density at the

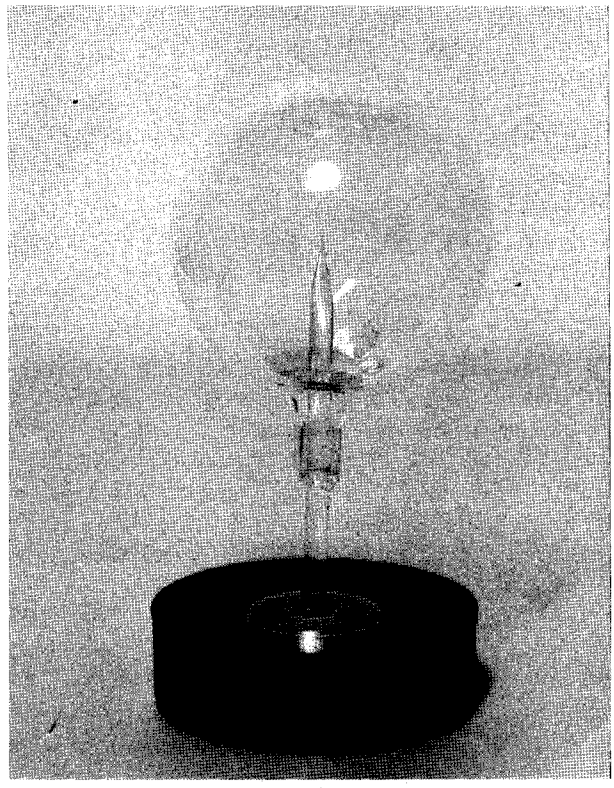

FIG. 3. Photograph of assembled bubble-target.

bubble surface is sufficiently low ($\lesssim 10^{11}$ W/cm^2) as to not produce plasma formation which would be strongly absorbing and would impede the laser pulse from reaching the target.

The target-absorbed laser energy appears as intense soft x-ray emission and expanding plasma. The very-low-energy portion of the x-ray spectrum (~100—1000-eV photons) will be strongly absorbed by the bubble, but the higher-energy photons will be transmitted, allowing x-ray pinhole photography as usual, though the pinhole must now be placed at a somewhat larger than normal distance from the target so as not to interfere with the plastic bubble.

The plasma ions from the laser-driven implosion are composed of the energetic tamper silicon, oxygen, and sodium ions and the deuterium-tritium fuel ions. The range tables of Northcliff and Schilling[12] indicate that all but the very-highest-energy "fast" ions[13] ($v > 2\times10^8$ cm/sec) are effectively absorbed by the plastic bubble.

Computer code calculations, using the KMS Fusion TRHYD code,[14] show that the tamper material which implodes the DT fuel expands at relatively low velocities ($\lesssim 5\times10^7$ cm/sec). This component of the target expansion material is quite effectively absorbed in the bubble.

The bubble is sufficiently thin to allow the DT reaction products from the core to be transmitted with little energy loss (provided the α's leave the tamper with $\gtrsim 2$ MeV).

It is clear from these considerations that the plastic bubble acts as a nuclear-particle filter, allowing α's and neutrons to be transmitted but partially or completely absorbing both the plasma x-ray flux and the ion flux. This is an advantage for nuclear-particle measurements since the x-ray and ion flux are effectively noise in scintillation detectors, for example. Another considerable advantage of the plastic bubble is the protection it affords to the delicate and expensive focusing optics.[9] A disadvantage, from the point of view of the plasma diagnostics, is that the usual plasma charge collector measurements, soft x-ray measurements, and differential calorimeter measurements[13] are impossible. A countervailing possibility is to use the plastic bubble as a pressure probe by measuring its radial acceleration by interferometric or holographic techniques. Alternatively, some holes could be cut into the bubble to sample the plasma flow.

The bubble target shown in Fig. 3 was irradiated in the KMS Fusion experimental chamber at about 0.20 TW. The bubble survived the vacuum pumpdown, the laser pulse, the target explosion, and the vacuum release. The bubble showed no signs of local damage. The charge collectors recorded no ion flux, and the total x-ray flux (as measured with thermoluminescent dosimeters) was done by a factor of 50 to 100 from a similar target with no bubble. An x-ray pinhole photograph was taken which indicated an imploded target. In this experiment, however, the neutron yield was low and no tamper activation was detected.

IV. ACTIVATION ANALYSIS

While many materials could be introduced to the pusher tamper for neutron activation, the glass-shell fusion target naturally contains a fair amount of silicon which has a relatively large cross section for neutron activation. Table I gives the atomic composition of the present KMS Fusion glass-shell targets. The nuclear reaction of primary interest is

$$_{14}\mathrm{Si}^{28}(n,p)_{13}\mathrm{Al}^{28} \rightarrow {}_{14}\mathrm{Si}^{28} + \beta^{-(2.85\ \mathrm{Mev})}$$

There is also some activation of Na by (n,p) and (n,α) reactions, but it can be neglected relative to the Si activity.

The plastic bubble containing the imbedded activated silicon is easily dissolved in various organic solvents. We have chosen to use acetone as the bubble solvent and have found that 20 ml of acetone very quickly (~1 sec) dissolves the bubble (with the imbedded glass target material at ~1 ppm by mass).

The acetone solution is conveniently counted in a Packard Tri-Carb liquid scintillation system,[15] in a Cerenkov counting scheme discussed by Haberer.[16] The Cerenkov lower energy limit for acetone is close to that of water, i.e., 260 keV, effectively discriminating against the tritium activity which is also present in the dissolved bubble.

Absolute counting efficiency calibrations have been performed using known quantities of Pr-144 (β end-point energy of 2.98 meV) and standard-size plastic bubbles dissolved in acetone. Typical background count rates are ~5 cpm for our experimental conditions.

The 20-ml acetone bubble solution is a convenient sample size for the standard health physics sample vials. We have used both polyethylene and boro-silicate glass vials with no difference in background.

As quickly as possible after the laser implosion experiment, the bubble is dissolved, inserted into the Tri-Carb and counted at 0.1-min intervals for about 4 min. The measured counts are least-squares fitted to the integral count equation to determine the total number of activated nuclei. The number of counts at time t after counting starts is given by

$$N(t) = \dot{N}_b t + \epsilon N_0 \exp(-t_0/\tau)[1 - \exp(-t/\tau)], \quad (1)$$

where N_b is the background count rate, ϵ is the detection efficiency, N_0 is the number of activated silicon nuclei, t_0 is the time after activation that counting begins, and τ is the decay time ($1.44t_{1/2}$) equal to 3.33 min for Al^{28} β decay.

TABLE I. Atomic composition of the present KMS Fusion glass-shell targets.

Element	at.%
Si	25.7%
O_2	59.2%
Na	13.2%
B	1.9%

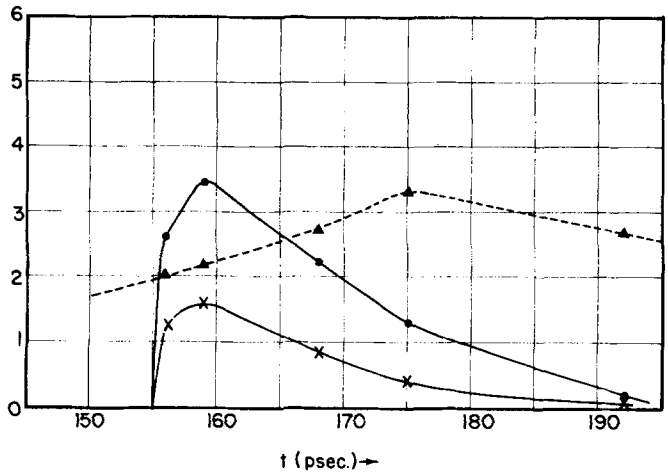

FIG. 4. TRHYD code calculation of the time history of ▲, $\int_{r_f}^{\infty}\rho(r,t)\,dr\times10^{4}$ g cm^{-2}; ×, $(dN/dt)\times10^{-18}$ neutron sec^{-1}; ●, $(dN/dt)\int_{r_f}^{\infty}\rho(r,t)\,dr\times10^{-14}$ g cm^{-2} neutrons sec^{-1}.

V. $\langle\rho R\rangle$ DATA REDUCTION

The number of activated nuclei produced is given by

$$N_0=\int_{t=0}^{t=\infty}\frac{dN_n(t)}{dt}\int_{r_f}^{\infty}n_{\mathrm{Si}}(r,t)\sigma_{\mathrm{Si}}\,dr\,dt,$$

where N_0 is the number of activated nuclei, $dN_n(t)/dt$ is the neutron generation rate, $n_{\mathrm{Si}}(r,t)$ is the number density of silicon nuclei in the tamper, σ_{Si} is the (n,p) cross section at 14 meV = 233 mb,[17] and r_f is the radius of DT-fuel–glass-tamper interface. The integrals are carried out over radius (r) and time (t). The silicon number density is directly proportional to the tamper mass density, the conversion factor (for the present glass composition) being 8.4×10^{21} silicon nuclei/g of glass. The neutron production rate dN_n/dt is a more sharply peaked function of time during the implosion than is the $\langle\rho R\rangle$ (or $n_{\mathrm{Si}}R$) function and therefore, the activation method preferentially samples the tamper $\langle\rho R\rangle$ at peak neutron generation time. This is seen clearly in Fig. (4) where we have separately plotted dN_n/dt, $\int_{r_f}^{\infty}\rho(r,t)\,dr$, and $(dN_n/dt)\int_{r_f}^{\infty}\rho(r,t)\,dr$ versus time in psec. These results were obtained using the KMS Fusion hydro code TRHYD.[14] As can be seen, the $\int_{r_f}^{\infty}\rho(r,t)\,dr$ peaks later than the maximum neutron generation rate, therefore the activation was mostly produced when the tamper ρR was about one-half its maximum value. This TRHYD calculation was for a 67-μm-diam glass-shell target with a 0.5-μm wall filled to a DT gas pressure of 30 atm, which absorbed 4.8 J of laser energy.

Using the values of $(dN_n/dt)\int_{r_f}^{\infty}\rho(r,t)\,dr$ from Fig. (4), a numerical integration gives

$$N_0=C\int_0^{\infty}\frac{dN_n}{dt}\int_{r_f}^{\infty}\rho(r,t)\,dr\approx C\left(6300\,\frac{\mathrm{g}}{\mathrm{cm}^2}\right),$$

where

$$C=(\sigma_{\mathrm{Si}})\,8.4\times10^{21}=2.3\times10^{-3}\ \mathrm{cm}^2/\mathrm{g},$$

so that $N_0=15$, with a total neutron yield of 1.9×10^{7} and an average tamper $\langle\rho R\rangle$ at the neutron production peak of $\sim2\times10^{-4}$ g/cm^2.

Pursuing this example, the 15 activated nuclei produce according to Eq. (1) the following data. Suppose $\epsilon=0.5$, $\dot{N}_b=5$ cpm, $t_0=0.5$ min, and $\tau=3.33$ min, the total count distribution after 2 min will consist of ten background counts and only three real counts. As this example shows, the activation method is just on the verge of crossing the detection threshold. The lack of a precise value for the silicon (n,p) cross section leaves the $\langle\rho R\rangle$ measurement inaccurate in the same ratio. However, at much higher neutron yields and higher $\langle\rho R\rangle$ values, the more precisely known oxygen activation cross sections are accessible, and as a result, a cross-section measurement relative to the oxygen can be made for silicon.

VI. CONCLUSIONS

We present here a new and powerful diagnostic measurement for laser-driven implosion experiments, by collecting all of the tamper material in macrospheres for radioactive analysis. The secondary advantages of the bubble technique, such as focusing optics protection, increased signal-to-noise ratio in α-particle measurements, and other plasma diagnostic possibilities (like interferometric measurements of the bubble momentum record) should make the technique of wide interest.

Unfortunately, the $\langle\rho R\rangle$ value and neutron yield of the present laser-driven implosion experiments are not quite high enough for a more quantitative comparison of measured and computed $\langle\rho R\rangle$; however, as the example presented indicates, the comparison should be possible in the near future.

Note added in manuscript. Experiments subsequent to the writing of this paper have shown a substantial radiation background activation produced by high-energy ($\frac{1}{2}$ meV) protons in the plasma ion expansion. Presently, experiments are being designed to use γ-ray spectrometry instead of the Cerenkov scheme to determine the number of activated tamper nuclei.

ACKNOWLEDGMENTS

The authors would like to thank R. Johnson for encouraging these experiments, R. Sigler for suggesting bubble blowing, L. Warren for painstakingly mounting the targets, and J. Trabalka for assistance in the activation analysis.

*This work was supported by the United States Energy Research and Development Administration.

[1]R. Johnson, F. Mayer, and G. Charatis, The Second International Conference on Plasma Science, Ann Arbor, Michigan, 1975, p. 122 (unpublished).
[2]J. Holtzrichter, H. Ahlstrom, E. Storm, and J. Swain, Ref. 1, p. 85.

[3]G. McCall, R. Godwin, and D. Giovanielli, Ref. 1, p. 81.
[4]D. Woodall, B. Arad, W. Friedman, L. Goldman, S. Letzring, M. Lubin, B. Nicholson, I. Pelah, J. Sources, J. Wilson, and B. Yaakobi, Ref. 1, p. 120.
[5]J. Nuckolls, L. Wood, A. Thiessen, and G. Zimmerman, Nature London 239, 139 (1972).
[6]K. Brueckner and S. Jorna, Rev. Mod. Phys. 46, 325 (1974).
[7]P. Hammerling and R. Osborn, KMS Fusion, Inc., unclassified internal document, Report No. KMSF-U148, 1972 (unpublished).
[8]A. Grosse, Sci. Am. **231**, 110 (1973).
[9]C. Thomas, Appl. Opt. 14, 126 (1975).
[10]G. Charatis, J. Downward, R. Goforth, B. Guscott, T. Henderson, S. Hildum, R. Johnson, K. Moncur, T. Leonard, F. Mayer, S. Segall, L. Siebert, D. Solomon, and C. Thomas, Plasma Physics and Controlled Nuclear Fusion Research (IAEA, Vienna, 1975), Vol. II.
[11]J. Downward, J. Appl. Phys. 46, 2147 (1975).
[12]L. Northcliffe and R. Schilling, Nucl. Data Tables 7, 233 (1970).
[13]F. Mayer, C. Cheng, and J. Downward, Bull. Am. Phys. Soc. 19, 910 (1974).
[14]The authors are grateful to Dr. R. Grandey for providing them with the TRHYD code results.
[15]Packard Instrument Co., Inc., 2200 Warrenville Road, Downers Grove, Ill. 60515.
[16]Atomwirtschaft 10, 36 (1965).
[17]ENDF/B-IV Library, *NNCSC Newsletter*, No. 74-4 (National Neutron Cross Section Center, Brookhaven National Laboratory, Upton, New York, July-August, 1974).